MOLECULAR AND CELLULAR BIOLOGY, Jan. 1997, p. 378–388 Vol. 17, No. 1
0270-7306/97/$04.00+0

Nop2p Is Required for Pre-rRNA Processing and 60S Ribosome Subunit Synthesis in Yeast

BO HONG, J. SCOTT BROCKENBROUGH, PEI WU, AND JOHN P. ARIS*

Department of Anatomy and Cell Biology, Health Science Center, University of Florida, Gainesville, Florida 32610-0235

Received 3 April 1996/Returned for modification 13 May 1996/Accepted 23 October 1996

To investigate the function of the nucleolar protein Nop2p in *Saccharomyces cerevisiae*, we constructed a strain in which *NOP2* is under the control of a repressible promoter. Repression of *NOP2* expression lengthens the doubling time of this strain about fivefold and reduces steady-state levels of 60S ribosomal subunits, 80S ribosomes, and polysomes. Levels of 40S subunits increase as the free pool of 60S subunits is reduced. Nop2p depletion impairs processing of the 35S pre-rRNA and inhibits processing of 27S pre-rRNA, which results in lower steady-state levels of 25S rRNA and 5.8S rRNA. Processing of 20S pre-rRNA to 18S rRNA is not significantly affected. Processing at sites A_2, A_3, B_{1L}, and B_{1S} and the generation of 5′ termini of different pre-rRNA intermediates appear to be normal after Nop2p depletion. Sequence comparisons suggest that Nop2p may function as a methyltransferase. 2′-*O*-ribose methylation of the conserved site $UmGm\Psi UC_{2922}$ is known to take place during processing of 27S pre-rRNA. Although Nop2p depletion lengthens the half-life of 27S pre-RNA, methylation of $UmGm\Psi UC_{2922}$ in 27S pre-rRNA is low during Nop2p depletion. However, methylation of $UmGm\Psi UC_{2922}$ in mature 25S rRNA appears normal. These findings provide evidence for a close interconnection between methylation at this conserved site and the processing step that yields the 25S rRNA.

Most of the steps of ribosome synthesis in eukaryotic cells occur in the nucleolus. Within the nucleolus, the rRNA gene is transcribed by RNA polymerase I into a large 35S rRNA precursor, which is processed via a series of steps into three mature rRNAs: 18S, 5.8S, and 25S (for reviews, see references 12 and 45). During processing, the assembly of ribosomal subunits begins as ribosomal proteins imported from the cytoplasm are assembled with pre-rRNAs and 5S RNA synthesized by RNA polymerase III. The large 60S subunit contains the 5S, 5.8S, and 25S rRNAs, whereas the small 40S subunit contains the 18S rRNA. Nucleolar proteins and small RNAs that are not part of mature ribosomes are thought to be localized to the nucleolus for the purpose of integrating and regulating assembly events (27, 34). Although nucleolar components involved in different steps of ribosome biogenesis have been identified and characterized, much remains to be learned about the specific functions of most nucleolar components.

The order in which pre-rRNAs are converted to mature rRNAs in *Saccharomyces cerevisiae* is relatively well understood (for reviews, see references 51 and 54). Proteins that are required for one or more processing steps include Dsr1p, Gar1p, Nsr1p, Nop1p, Nop4p/Nop77p, Rrp1p, and Sof1p (6, 15, 20, 30, 35, 37, 46, 49). Of these proteins, Nop4p/Nop77p is the only known nucleolar protein for which depletion or mutation results in processing defects that are greatest for the pathway leading to synthesis of 25S rRNA (7, 46). In addition to processing, rRNAs are subject to covalent modification, including methylation and pseudouridylation (for a review, see reference 29). With respect to methylation, the majority of methylation sites have been identified in mature rRNAs from a number of prokaryotic and eukaryotic species, and the known sites of methylation are distributed in mature rRNAs in a nonrandom, evolutionarily conserved manner (31). In the fully folded rRNAs, methylation sites are brought together into functionally important regions within the ribosome, suggesting a role for methylation in ribosome function (29, 33). Recently, small nucleolar RNAs have been shown to play a central role in the selection of methylation sites in rRNA (22, 36). However, the importance of pre-rRNA methylation for processing and ribosome biogenesis remains unclear. Methylation of yeast pre-rRNA does not appear to be required for processing events (50). On the other hand, a yeast *pet56* mutant, which fails to methylate a conserved position in mitochondrial 21S rRNA, is deficient in formation of the large ribosomal subunit in mitochondria (44). The methylase Dim1p is required for processing, not because of its function in 18S rRNA dimethylation per se but because its association with the preribosomal particle appears to be monitored by the cell (28). In mammalian cells, pre-rRNA processing is sensitive to the inhibition of pre-rRNA methylation (9, 47, 53). These results from different experimental systems suggest that the relationship between processing and methylation may differ among eukaryotes and that certain pre-rRNA processing and modification events may be coupled in the pre-rRNA processing pathway while others may not.

Nop2p is a yeast nucleolar protein that is specifically upregulated during the onset of growth and is homologous to nucleolar protein p120 (10). p120 is a human proliferation marker that is predicted to function as a methylase (14, 25). In this study, we demonstrate that Nop2p is required for synthesis of the 60S ribosomal subunit and processing of the 27S precursor to mature 25S and 5.8S rRNAs. Furthermore, we have explored the relationship between rRNA processing and methylation to determine if these two events are interdependent during synthesis of the large subunit. The fact that depletion of Nop2p results in reduced processing of 27S pre-rRNA and leads to undermethylation of the 27S pre-rRNA at the conserved loop containing $UmGm\Psi UC_{2922}$ suggests that process-

* Corresponding author. Phone: (352) 392-1873. Fax: (352) 392-3305. E-mail: johnaris@college.med.ufl.edu.

TABLE 1. Yeast strains used in this study

Strain	Genotypic description	Source
L4717	*MAT***a** *ade2 can1-100 his3-11,15 leu2-3,112 trp1 ura3-1*	C. A. Styles, G. R. Fink
YBH3	L4717 *nop2*::*LEU2* pJPA40	This study
YBH5	L4717 *nop2*::*LEU2* pBH47	This study
YBH12	L4717 pJPA40	This study

ing and methylation events during conversion of 27S pre-rRNA to 25S rRNA are tightly coupled.

MATERIALS AND METHODS

Strains, plasmids, and microbiological methods. *S. cerevisiae* strains and plasmids used in this study are described in Tables 1 and 2, respectively. Yeast cells were grown at 30°C either in YPD or YPGal (1% yeast extract–2% peptone with 2% glucose or galactose, respectively) or in SD or SGal synthetic minimal medium (0.67% yeast nitrogen base with 2% glucose or galactose, respectively, and required supplements) as described previously (41). Methionine was absent from synthetic media. For [^{3}H]uracil labeling, the concentration of uracil in synthetic media was reduced to one-third the normal amount (41). DNA was transformed into yeast cells by the lithium acetate method (19). Plasmid shuffling was done by the method of Sikorski and Boeke (42), with 1 mg of 5-fluoroorotic acid (5-FOA) per ml (7). *Escherichia coli* DH5α was used for routine maintenance and preparation of plasmids and was grown in LB medium (3).

Construction of a *nop2*::*LEU2 GAL-NOP2* haploid strain. Previously, we demonstrated that *NOP2* was an essential gene by replacing 755 bp of the *NOP2* open reading frame (ORF) (~40% of 1,857 bp) with *URA3* (10). We sought to construct another disruption in which all of the *NOP2* ORF was replaced in order to eliminate the possibility of recombination between the chromosome and the complementing plasmid. However, we found the disruption of all of *NOP2* by conventional methods to be problematic. The approach we found to be successful was to disrupt *NOP2* in a haploid strain carrying a plasmid-borne *NOP2* gene. For this, plasmid pBH45 was created by replacing part of the 5′ noncoding region and 92% of the *NOP2* ORF between *Bam*HI and *Hin*dIII with a *Bam*HI-*Hin*dIII *LEU2* fragment from pJJ282 (21). L4717 was transformed to Ura$^+$ with plasmid pJPA40 to yield YBH12 (Table 1). A *Cla*I-*Bgl*II *nop2*::*LEU2* disruption fragment from pBH45 was used to transform YBH12. Two 5-FOA-sensitive isolates (YBH3 and YBH4) obtained from Leu$^+$ Ura$^+$ transformants were analyzed by Southern blotting as previously described (10). To introduce plasmid-borne *GAL-NOP2* into this background, pBH46 and pBH47 were constructed (Table 2). Plasmid shuffling was used to exchange pBH47 for pJPA40 in YBH3, and Trp$^+$ transformants were streaked onto SGal containing 5-FOA. Several isolates grew very slowly on dextrose media, forming small (0.2- to 0.4-mm) colonies after 3 to 5 days of growth on YPD plates at 30°C (data not shown). One isolate, YBH5, was used for further experiments.

Nop2p depletion, SDS-PAGE, and immunoblotting. YBH5 was grown at 30°C in liquid YPGal medium until mid-log phase (an optical density at 600 nm [OD_{600}] of 0.25 to 0.5) and washed with water, and equal volumes of cells were transferred to YPD or YPGal. Cultures were grown at 30°C and diluted with prewarmed medium when OD_{600} values reached 0.6 to 0.8. Total cellular protein was extracted in the presence of trichloroacetic acid, precipitated, separated on a 10.5% polyacrylamide gel by sodium dodecyl sulfate-polyacrylamide gel electrophoresis, and analyzed by immunoblotting with affinity-purified polyclonal antibody APpAb3 against Nop2p (10). Monoclonal antibody 1G1 (2), which is specific for Pab1p, was used subsequently on the same blot.

Ribosome and polysome analysis. Ribosomal subunits, monosomes, and polyribosomes were analyzed, with minor modifications, according to the method of Baim et al. (4). Cells grown in YPD were collected at mid-log phase (OD_{600} = 0.8 to 1.0). The cycloheximide stock solution was freshly prepared. Lysates were stored at −70°C without any effect on the ribosomal profiles, compared with those of freshly prepared lysates. A 15 to 50% (wt/vol) sucrose gradient was centrifuged at 40,000 rpm for 2.5 h at 4°C in an SW41Ti rotor and analyzed with an absorbance detector set at 254 nm.

Pulse-chase analysis of pre-rRNA and rRNA formation. Fresh overnight cultures were diluted into SGal, grown at 30°C for two to three doublings, washed with water, and diluted into 50 ml of SD medium at a density sufficient to yield an OD_{600} of 0.6 to 0.8 at the end of the depletion time course. Cells were collected by centrifugation, resuspended in 5 ml of SD, pulse-labeled for 3 min with 250 μCi of [*methyl*-^{3}H]methionine or [^{3}H]uracil at 25°C, and chased with methionine (5 mM) or uracil (2 mM). At each time point, 1 ml was mixed with ice and centrifuged for 30 s, and cell pellets were immediately frozen in dry ice and stored at −70°C. Total RNA was extracted by a hot-phenol method (24) or a glass bead method (10), with indistinguishable results.

To improve the detection of pre-rRNAs and rRNAs, [^{3}H]uracil-labeled RNA was treated with oligo(dT)-cellulose before gel separation. RNA samples were diluted to 25 μl with diethyl pyrocarbonate-treated double-distilled water, heated to 65°C for 10 min, and chilled on ice. Buffer (100 μl of 0.5 M LiCl–10 mM Tris-HCl [pH 7.45]–1 mM EDTA–0.1% SDS) was added, and the mixture was transferred to a microcentrifuge tube containing 20 μl of wet, packed oligo(dT)-cellulose (Boehringer Mannheim). The oligo(dT)-cellulose was freshly washed with alkali, double-distilled water, and buffer as described previously (3). After 30 min of gentle agitation at 25°C, the oligo(dT)-cellulose was pelleted. The supernatant was transferred to a fresh tube, and the RNA was ethanol precipitated, washed, and dried.

RNA samples were separated on a 1.2% agarose–glyoxal gel (3), which was treated with En^{3}Hance according to the instructions of the supplier (Du Pont NEN) and exposed to preflashed X-ray film. The amounts of [*methyl*-^{3}H]methionine radioactivity loaded per lane were ~8,000 cpm for YBH5 and ~50,000 cpm for L4717. The amounts of [^{3}H]uracil radioactivity were ~100,000 cpm per lane for YBH5 and ~500,000 cpm per lane for L4717.

Northern analysis. Total RNA was separated on a 1.2% agarose–glyoxal gel, transferred to a Hybond nylon membrane (Amersham), probed with ^{32}P-labeled oligonucleotides, and exposed to X-ray film. Oligonucleotides complementary to regions of rRNAs (see depiction in Fig. 4) are as follows: AGCCATTCGCAG TTTCACTG (oligonucleotide 1), GCACAGAAATCTCTCACCGT (oligonucleotide 2), TCCAGTTACGAAAATTCTTG (oligonucleotide 3), GCCTAGA CGCTCTCTTCTTA (oligonucleotide 4), and TACTAAGGCAATCCGGT TGG (oligonucleotide 5).

Primer extension. Primer extension was done with oligonucleotides 3, 5, and 9 by a modification of a previously described method (5). The sequence of oligonucleotide 9 is CATCCAATGAAAAGGCCAGC (see Fig. 4). Total RNA was extracted from L4717 or YBH5 grown on SGal as described above and transferred to SD for 8.5 h. Although equal amounts of cells (as determined by the OD_{600} values) were extracted, the yield of RNA from YBH5 was approximately fivefold less than from L4717, based on A_{260} measurements. Equal amounts of RNA from L4717 and YBH5 (as determined by A_{260} measurements) were always analyzed in parallel. Approximately 1 μg of RNA and 2 pmol of primer in 25 mM Tris-HCl (pH 8.3)–25 mM KCl–5 mM $MgCl_2$–5 mM dithiothreitol–0.25 mM spermidine were denatured at 70°C for 10 min and annealed at 42°C for 20 min. Labeling was done for 1 min at 42°C after the addition of the following: 4 μM (each) dCTP, dGTP, and dTTP; 25 μCi of [α-^{35}S]dATP; 5 U of avian myeloblastosis virus reverse transcriptase (Promega); and 20 U of RNase Block II (Stratagene). Extension was done for 10 min at 42°C after addition of all four deoxynucleoside triphosphates at 1 mM each. The reaction mixture was placed on ice and adjusted to 10 mM EDTA, and nucleic acids were precipitated with ethanol prior to electrophoresis by 8 M urea–6% PAGE.

RNase protection assay. RNase protection was done by a modification of a previously described method (40). RNA was extracted from L4717 or YBH5 grown in SD for 8.5 h, pulse-labeled with [*methyl*-^{3}H]methionine for 3 min, and chased for 4 min, as described above. [^{3}H]RNA from ~7 OD_{600} units of culture (~30 pmol of RNA) plus 300 pmol of oligonucleotide probe was denatured in 40% formamide–40 mM piperazine-*N*,*N*′-bis(2-ethanesulfonic acid) (PIPES)-HCl (pH 6.4)–400 mM NaCl–1 mM EDTA for 15 min at 85°C. The oligonucleotides used for protection are as follows: CGCATAGACGTTAGACTCCTTG GTCCGTGTTTCAAGACGG (oligonucleotide 6), CCCTATTAGTGGGTGA ACAATCCAACGCTTACCG (oligonucleotide 7), and CGGTCTAAACCCAG CTCATGTTCCCTATTAGTGGG (oligonucleotide 8) (see Fig. 4). Comparison of different hybridization conditions revealed that 4 h at 60°C was optimal. After cooling to 25°C, single-stranded RNA was digested with RNase A (20 μg/ml) and RNase T_1 (3 μg/ml) freshly added to 300 mM NaCl–10 mM Tris-HCl (pH 7.5)–5 mM EDTA. Digests were inactivated with SDS and proteinase K, supplemented with 10 μg of yeast tRNA, extracted with phenol-chloroform, ethanol precipitated, washed with 70% ethanol, and dried.

The protocol for partial digestion with RNase T_1 was a modification of the

TABLE 2. Plasmids used in this study

Plasmid	Relevant functional DNA	Comments
pBH46	*GAL10-NOP2 URA3 CEN6*	*Bam*HI-*Xho*I fragment containing *NOP2* from pJPA20 (10) cloned in the same sites of pRD53 (10a)
pBH47	*GAL10-NOP2 TRP1 CEN6*	*Sac*I-*Xho*I fragment containing *GAL10-NOP2* from pBH46 cloned in the same sites in pRS314 (43)
pJPA40	*NOP2 URA3 CEN6*	*Hpa*I-*Kpn*I fragment (3,027 bp) containing *NOP2* plus 715 bp of 5′ flanking sequence and 456 bp of 3′ flanking sequence from pJPA30 (10) cloned into pRS316 (43); size, 7.85 kb

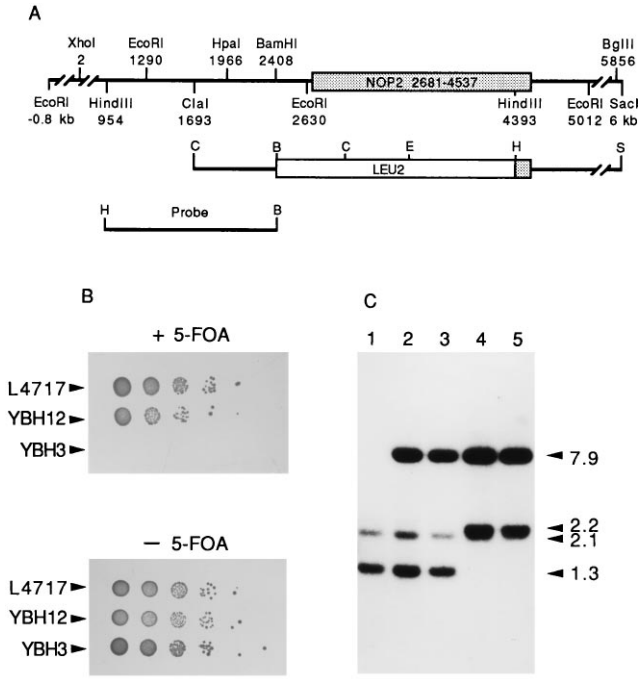

FIG. 1. Construction of a conditionally lethal *GAL-NOP2* strain. (A) Restriction maps of the *NOP2* locus, the *nop2*::*LEU2* disruption fragment, and the probe used for Southern blotting. (B) The viability of the *nop2*::*LEU2* strain, YBH3, was dependent on plasmid-borne *NOP2*. Serial dilutions (1/10 each) of L4717, YBH12, and YBH3 (see Table 1) were grown on SD medium with or without 5-FOA. (C) Southern analysis of *Eco*RI digests of genomic DNA from L4717 (lane 1), two *NOP2* isolates carrying pJPA40 (lanes 2, 3), and two disruptions, YBH3 (lane 4) and YBH4 (lane 5), carrying pJPA40. The 7.9-kb band corresponds to linearized plasmid.

procedure of Knapp (23). [^{3}H]RNA from ~1 OD_{600} unit of culture was resuspended in 10 mM Tris-Cl (pH 7.0)–10 mM $MgCl_2$–100 mM KCl and digested with 0.1 U of RNase T_1 (Sigma) per μl for 10 min at 37°C.

Samples were electrophoresed on 12% polyacrylamide–7 M urea gels by a standard method (3). Gels were fixed and treated with En^{3}Hance according to the instructions of the manufacturer (Du Pont NEN). Following fluorography, sections of dried gels were excised and digested with 1 ml of Scintigest (Fisher Scientific) at 37°C overnight in tightly capped glass vials. Samples were neutralized by the addition of 100 μl of glacial acetic acid, mixed with Scintiverse E (Fisher Scientific), and subjected to scintillation counting for a sufficient length of time (0.5 to 8 h per determination) to yield an error of ±2% of the mean disintegrations per minute at a confidence level of 95%.

RESULTS

Repression of *NOP2* decreases the growth rate and the steady-state level of 25S rRNA. To examine the consequences of depleting intracellular levels of Nop2p, *NOP2* was placed under the control of the *GAL10* promoter in plasmid pBH47 and shuffled into YBH3 to create YBH5 (Table 1). To create YBH3, it was necessary to disrupt *NOP2* in a haploid strain carrying a plasmid-borne *NOP2* gene. Approximately 90% of the *NOP2* ORF and part of the 5′ noncoding region in YBH3 is replaced with *LEU2* (Fig. 1A). YBH3 is sensitive to 5-FOA, whereas L4717 and YBH12 (Table 1) form colonies on SD plates containing 5-FOA (Fig. 1B). Disruption of genomic *NOP2* was confirmed by Southern analysis. *Eco*RI digestion of gDNA from YBH3 (Fig. 1C, lane 4) and another 5-FOA-sensitive isolate (YBH4) (Fig. 1C, lane 5) revealed a 2.2-kb band but no 1.3-kb band, indicative of the correct integration.

To deplete Nop2p, YBH5 cells were shifted from YPGal to YPD medium. During the first 8 h in YPD, YBH5 grew at a rate similar to that of these cells in YPGal (Fig. 2A). However, after 8 h in YPD, cell growth was impaired and the generation time increased fivefold from ~2.5 h to ~12.5 h (Fig. 2A). Immunoblotting with anti-Nop2p confirmed that Nop2p was indeed depleted (Fig. 2B). At 2 h after the medium shift, the Nop2p level was significantly reduced, and after 4 h in YPD, Nop2p was not detectable (Fig. 2B). By comparison, levels of the cytoplasmic poly(A) binding protein encoded by *PAB1* were essentially unchanged during growth in YPD (Fig. 2B). India ink staining of the immunoblot in Fig. 2 showed that very similar amounts of protein were loaded in each lane (data not shown). Thus, growth of YBH5 on glucose-containing medium substantially depletes the cells of Nop2p.

To explore the possibility that Nop2p was involved in ribosome biogenesis, the levels of 18S and 25S rRNAs from YBH5 grown on YPGal or YPD were compared (Fig. 2C). After growth in YPD for 28 h, the abundance of the 25S rRNA was

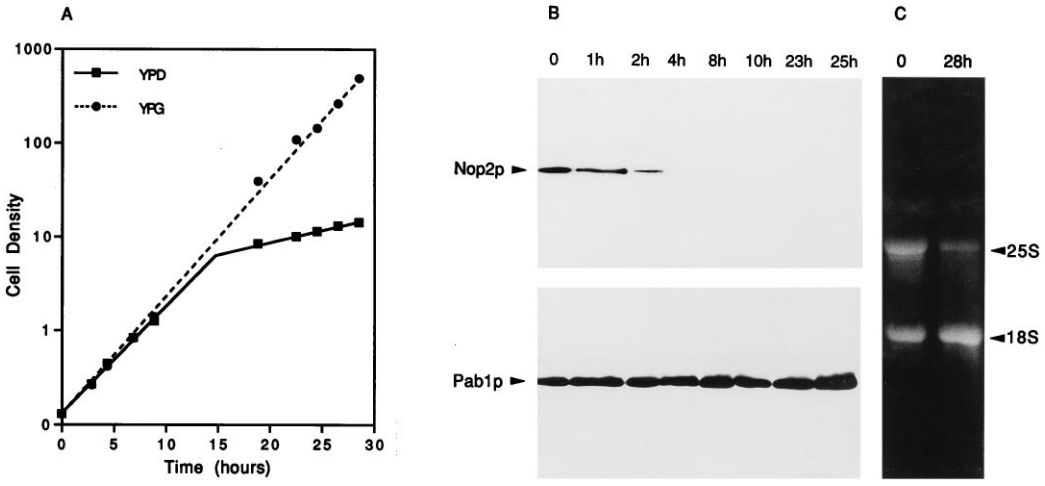

FIG. 2. Effect of Nop2p depletion on cell growth rate and levels of 25S rRNA. (A) YBH5 (*GAL-NOP2*) cells were transferred to either YPD or YPGal media (0 time) and diluted as needed to maintain logarithmic growth, and cell densities (OD_{600}s) were measured. (B) Analysis of Nop2p level in YBH5 cells grown in YPD. Total cellular protein was collected at the indicated time after shifting to YPD and analyzed by immunoblotting with affinity-purified anti-Nop2p antibody or antibody to the cytoplasmic poly(A) binding protein Pab1p. (C) Total RNA was extracted from YBH5 after growth on YPD for 0 or 28 h, separated on an agarose-glyoxal gel, and stained with ethidium bromide.

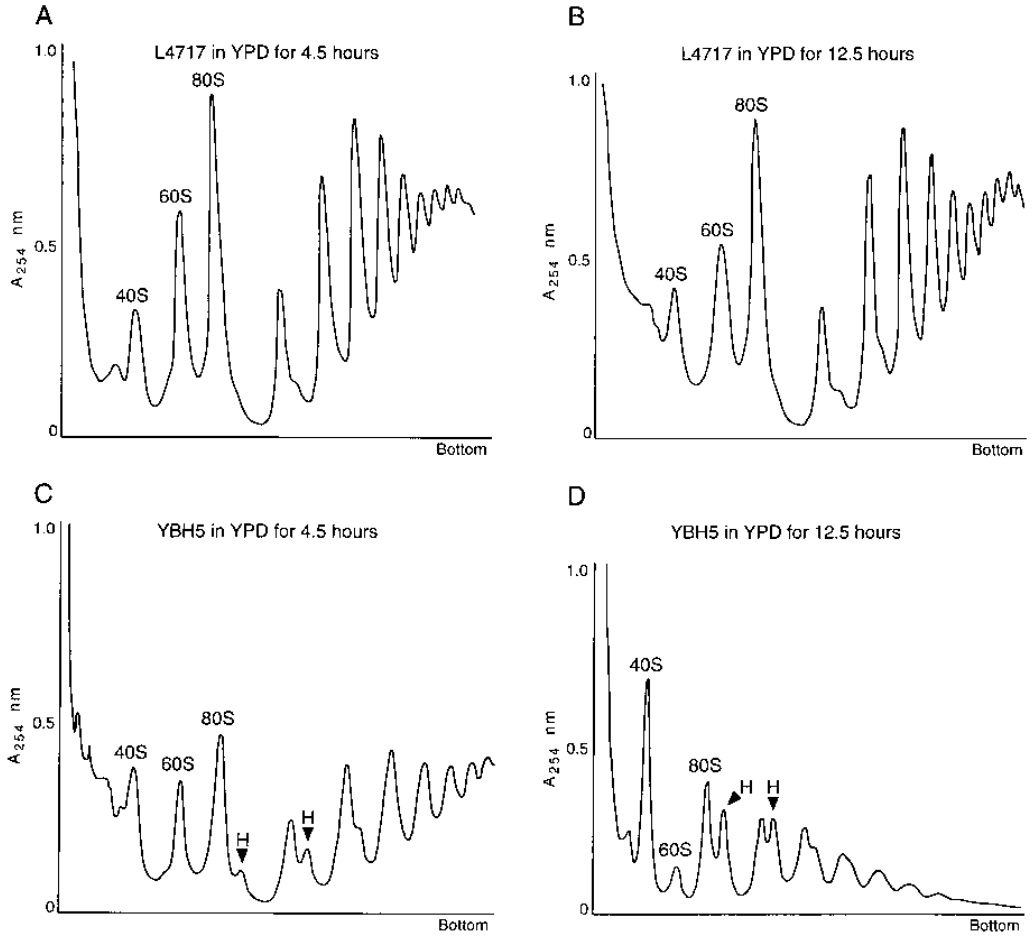

FIG. 3. Analysis of levels of ribosomal subunits, monosomes, and polysomes. L4717 (*NOP2*) (A and B) and YBH5 (*GAL-NOP2*) (C and D) cells were grown in YPGal, shifted to YPD medium for 4.5 (A and C) or 12.5 (B and D) h, and analyzed by using sucrose density gradients. Subunits, ribosomes, and polyribosomes were detected by measurement of A_{254} values. Preinitiation complexes are labeled H (for halfmer ribosomes).

reduced by more than half (Fig. 2C). In contrast, the abundance of the 18S rRNAs appears to be unaffected (Fig. 2C). This suggests that Nop2p depletion leads to reduced synthesis and/or stability of the large ribosomal subunit.

To rule out the possibility that the effects of Nop2p depletion can be attributed to cell death, cell viability after depletion was estimated. For this, cells were collected from YPD and YPGal media after 0, 1, 2, 4, 8, 10, 23, and 25 h of growth and diluted to 0.001 OD_{600} unit, and equal volumes were spread onto YPGal and YPD plates. The numbers of colonies appearing after 3 days on YPGal (2- to 3-mm diameter) and 5 days on YPD (~0.5-mm diameter) indicated that the viability of YBH5 during depletion is high, ranging from 97% at 2 h to 90% at 25 h (data not shown). Since at least 90% of YBH5 cells grown in YPD were viable at the time points assayed in the experiment whose results are shown in Fig. 2, the reduction in the 25S rRNA level was not a secondary effect of cell death.

Depletion of Nop2p causes a defect in the synthesis of 60S subunits. The reduction in steady-state levels of 25S rRNA upon Nop2p depletion, coupled with our previous observation that Nop2p is located primarily in the nucleolus, suggested a role for Nop2p in ribosome synthesis, perhaps at the level of the 60S subunit. To explore such a role for Nop2p, polysomes, ribosomes, and ribosomal subunits from cells depleted of Nop2p were analyzed on sucrose density gradients.

YBH5 and L4717 were grown on YPGal, shifted to YPD, and grown on that medium for either 4.5 or 12.5 h. After 4.5 h of growth in YPD, L4717 shows a typical profile of 40S and 60S subunits, the 80S monosome, and polysome peaks corresponding to 2 to 10 ribosomes (Fig. 3A). YBH5, however, shows noticeable reductions in the 60S, 80S, and polysome peaks after 4.5 h (Fig. 3C). The 40S peak is not significantly affected after 4.5 h of depletion. Furthermore, additional, small peaks follow the 80S and first two polysome peaks (Fig. 3C). The relative sedimentation values of these additional peaks correspond to "halfmer" polysomes, which represent 43S preinitiation complexes composed of mRNA, the 40S subunit, and initiation factors (17). Since the growth rate of the Nop2p-depleted cells is similar to that of nondepleted cells during the first 8 h after the shift to glucose (Fig. 2A), these polysome profile results are not a secondary effect attributable to the reduced growth rate.

After 12.5 h in YPD, the L4717 profile appears to have changed little from that for the 4.5-h time point (Fig. 3B). However, in YBH5 at 12.5 h, the 60S subunit peak is dramatically reduced, and this is accompanied by an accumulation of the 40S subunit (Fig. 3D). The 80S peak is substantially reduced, which is consistent with the deficit of 60S subunits. Halfmer polysome peaks are prominent (Fig. 3D), which is consistent with a reduction in the pool of free 60S subunits. As

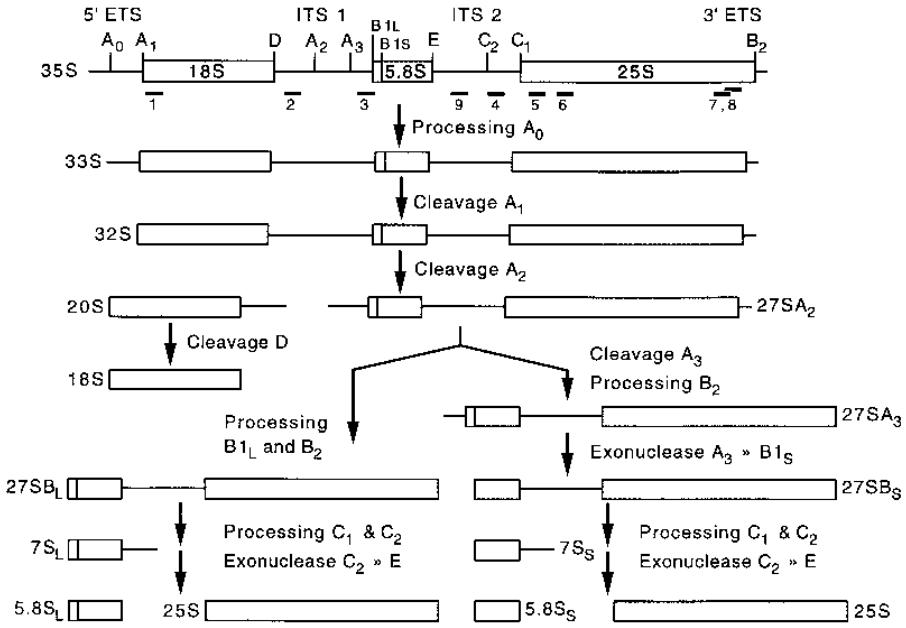

FIG. 4. The major pre-rRNA processing pathways in *S. cerevisiae*. The 35S primary transcript contains 18S, 5.8S, and 25S rRNA sequences separated by ITS1 and ITS2. Externally transcribed spacers precede (5′ ETS) and follow (3′ ETS) these sequences. The processing of the 35S precursor to mature rRNA involves endonucleolytic and exonucleolytic steps at specific sites as indicated. The 35S precursor is rapidly converted to a 33S pre-rRNA by cleavage at A_0 (not shown). Cleavage D is thought to occur in the cytoplasm. The relative positions of oligonucleotides 1 to 9 are indicated.

an additional control, strain YBH3 (Table 1) was analyzed after 12.5 h of growth on YPD, and the polysome profile was virtually identical to the profile of L4717 (data not shown).

Nop2p is required for processing of the 27S pre-rRNA. One explanation for reductions in levels of 25S rRNA and 60S ribosomal subunits during Nop2p depletion is a requirement for Nop2p in the pre-rRNA processing pathway leading to 25S rRNA synthesis. This processing pathway is diagrammed in Fig. 4. To investigate processing of pre-rRNA, cells were grown in SGal, shifted to SD for 8.5 h, pulse-labeled with [*methyl*-^{3}H]methionine, and chased for different lengths of time.

In L4717 cells, the 35S precursor disappeared within the first 2 min of the chase (Fig. 5B), indicating normal, rapid processing into 27S and 20S intermediates. By 4 min of chasing, most of the 27S and 20S intermediates were processed to 25S and 18S rRNAs. At 8 min of chasing only mature rRNAs were visible (Fig. 5B).

In Nop2p-depleted YBH5 cells, 35S and 32S pre-rRNAs are visible after 2 min of chasing, showing evidence for a reduced rate of processing (Fig. 5A). After 4 min of chasing only a small amount of the 27S intermediate is processed into 25S rRNA, in contrast to the almost complete conversion of 27S to 25S in L4717 at this time. Also, by 4 min of chasing in Nop2p-depleted cells, a significant amount of 20S precursor is converted to 18S product (Fig. 5A). At 8 min of chasing, slow processing of the 27S intermediate remained evident, although synthesis of the 18S rRNA appeared complete, as in L4717 (Fig. 5A). In two other experiments, ~10 and ~25% of 27S was processed to mature 25S rRNA by 8 min of chasing (data not shown).

To rule out the possibility that depletion of Nop2p causes virtually complete demethylation of the 25S rRNA and that this accounts for the absence of the 25S band after labeling with [*methyl*-^{3}H]methionine, pulse-chase labeling was done with [^{3}H]uracil. L4717 and YBH5 were grown in SD medium for 8.5 h. Because of slower rates of uracil incorporation and differences in intracellular pool size, longer chase times are required in uracil pulse-chase experiments for visualization of precursor-product relationships (see reference 52). Thus, at 2 min of chasing in L4717, the 27S and 20S pre-rRNAs remain prominent, and 8 min of chasing is required for visualization of the 25S and 18S rRNAs (Fig. 6B). In YBH5, however, at 16 min of chasing, the 27S pre-rRNA remains more abundant than the 25S rRNA (Fig. 6A). At 32 min of chasing, the majority of 27S has been processed, but a reduction in the rate

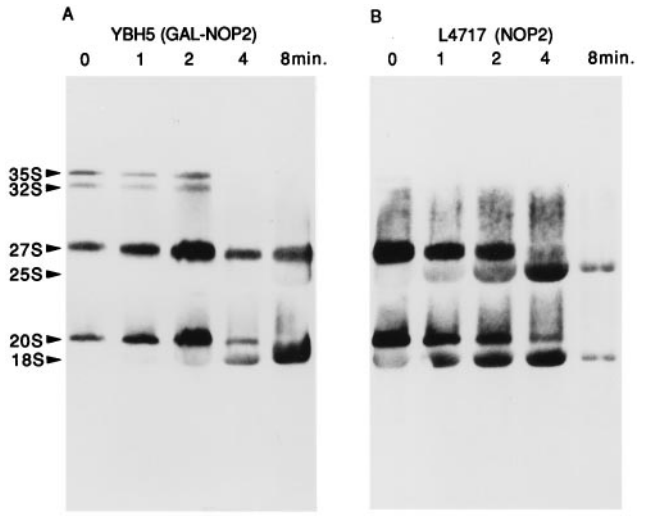

FIG. 5. Pulse-chase labeling analysis of pre-rRNA processing using [*methyl*-^{3}H]methionine. YBH5 (*GAL-NOP2*) (A) and L4717 (*NOP2*) (B) were grown in SGal, shifted to SD for 8.5 h, pulse-labeled with [*methyl*-^{3}H]methionine, and chased with excess methionine for 0, 1, 2, 4, and 8 min. Total RNA was extracted, separated on an agarose-glyoxal gel, and detected by fluorography. Approximately one-third of the L4717 8-min sample was loaded on the gel.

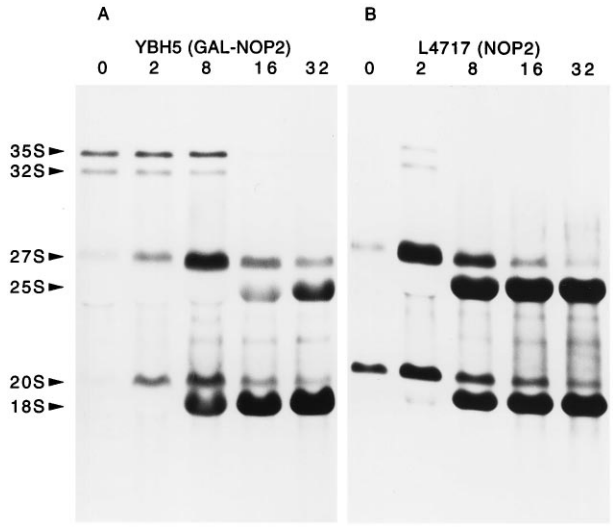

FIG. 6. Pulse-chase labeling analysis of pre-rRNA processing using [^{3}H]uracil. YBH5 (*GAL-NOP2*) (A) and L4717 (*NOP2*) (B) were grown in SGal, shifted to SD for 8.5 h, pulse-labeled with [^{3}H]uracil, and chased with excess uracil for 0, 2, 8, 16, and 32 min. Prior to agarose-glyoxal gel electrophoresis, samples were treated with oligo(dT)-cellulose.

of processing is clearly evident by the persistence of the 27S pre-rRNA (Fig. 6A). In contrast, processing of 20S pre-rRNA to 18S rRNA is not significantly affected. These results are consistent with the inhibition of processing of 27S pre-rRNA during Nop2p depletion and argue against wholesale demethylation of the 25S rRNA.

These results indicate that processing of 27S pre-rRNA continues at a greatly reduced rate during depletion of Nop2p. At 32 min of chasing in YBH5, processing of 27S pre-rRNA is greatly reduced but not abolished (Fig. 6A). One possibility is that the low rate of processing of 27S pre-rRNA may be due to a small amount of Nop2p synthesized by basal-level expression from the *GAL10* promoter.

The effect of Nop2p depletion on 27S pre-rRNA processing predicts that the formation of 5.8S rRNA should be affected in the same manner. We examined 5.8S rRNA synthesis by [^{3}H] uracil pulse-chase labeling of YBH5 after growth on SD for 8.5 h (Fig. 7). The synthesis of 5.8S rRNA is reduced by Nop2p depletion, and after 30 min of chasing, the amount of 5.8S rRNA is significantly lower than in L4717. However, the formation of 5S rRNA, an RNA polymerase III transcript, was not significantly affected by depletion of Nop2p (Fig. 7).

27SA and 27SB rRNA precursors accumulate during Nop2p depletion. To determine the steady-state levels of pre-rRNA and rRNA in Nop2p-depleted cells, Northern blotting analysis was done with oligonucleotide probes (see Fig. 4 for positions of the probes). YBH5 cells depleted of Nop2p for 4.5 or 8 h accumulate a significant amount of the 35S and 32S precursors compared to cells at the 0-h time point and compared to YBH3 and L4717 (Fig. 8A to C). Steady-state levels of 27S pre-rRNA also increase during Nop2p depletion (Fig. 8A and B). The most abundant form that accumulates upon depletion is the 27SB pre-rRNA. A smaller amount of 27SA accumulates as well; this is seen with the use of oligonucleotide 3 as a probe to the 3′ end of internally transcribed spacer 1 (ITS1) (Fig. 8B). Longer time periods of Nop2p depletion have been examined by Northern blotting and show reductions in levels of 18S and 25S rRNAs and pre-rRNAs (data not shown).

In contrast to effects on 27S levels, no accumulation of 20S rRNA is detected after depletion of Nop2p (Fig. 8C). On the contrary, a small decrease in the relative level of 20S rRNA is visible at 8 h of Nop2p depletion (Fig. 8C). This may be explained by a reduction in the processing of 35S and 32S precursors to the 20S and 27S intermediates. Interestingly, an unusual processing intermediate, the 23S rRNA, becomes somewhat more prevalent with Nop2p depletion. The 23S pre-rRNA is generated by cleavages A_0 and A_3 (Fig. 4) as part of an alternative pathway for the production of the 18S rRNA (39). This alternative pathway is thought to be a minor one in wild-type yeast cells. Increased amounts of the 23S rRNA have been shown to be a consequence of the depletion of other nucleolar proteins. Depletion of Nop1p (49), Gar1p (15), or small nucleolar RNA U3 (48) caused the accumulation of 23S rRNA. However, depletion of Nop2p has only a modest effect on the level of the 23S intermediate.

Similar amounts of RNA were compared side by side in this analysis, as shown by the relative intensities of the 18S and 25S rRNAs from YBH5, YBH3, and L4717 (Fig. 8D). The accumulation of pre-rRNAs at 8 h of Nop2p depletion is dramatic considering that this lane contains relatively less RNA than the

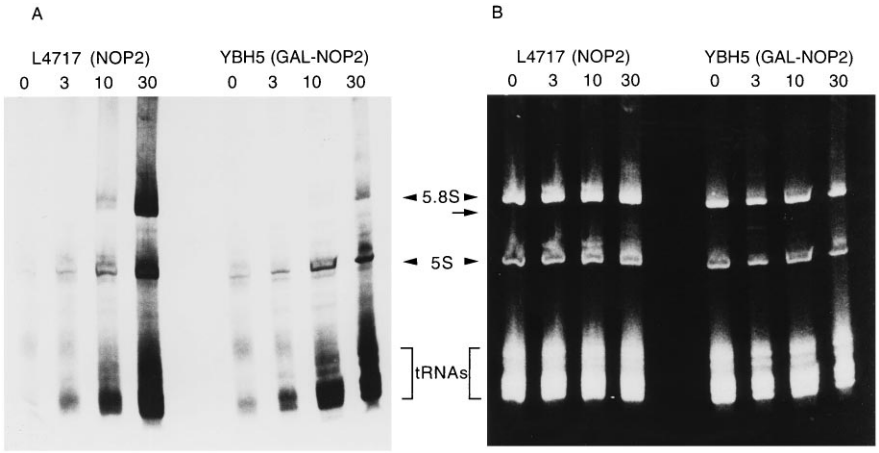

FIG. 7. Pulse-chase analysis of 5.8S and 5S rRNA synthesis with [^{3}H]uracil. YBH5 (*GAL-NOP2*) and L4717 (*NOP2*) were grown in SGal, shifted to SD for 8.5 h, pulse-labeled with [^{3}H]uracil, and chased with excess uracil for 0, 3, 10, and 30 min. RNAs were separated in a 12% polyacrylamide–urea gel and visualized by fluorography (A) or by ethidium bromide staining (B). The position of a 0.15-kb RNA standard (arrow) is indicated.

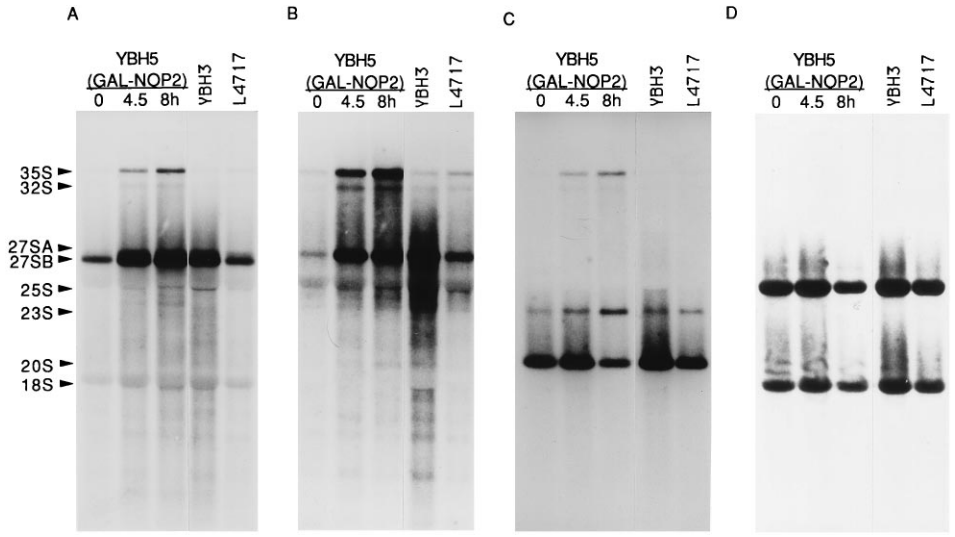

FIG. 8. Northern analysis of steady-state levels of precursor and mature rRNAs. Total RNA was extracted from YBH5 (*GAL-NOP2*) cells collected after 0, 4.5, and 8 h of growth on YPD. YBH3 and L4717 cells were grown in YPD. RNAs were separated on an agarose-glyoxal gel, transferred to a nylon membrane, and hybridized to ^{32}P-labeled oligonucleotides. (A) Oligonucleotide 4; (B) oligonucleotide 3; (C) oligonucleotide 2; (D) oligonucleotides 1 and 5. See Fig. 4 for the positions of oligonucleotides 1 to 5.

other lanes (Fig. 8D). Also, the 32S and 35S pre-rRNAs are barely, or not at all, detectable in control samples, which is consistent with a generalized reduction in metabolic flow through the processing pathway as a result of impairment of 27S pre-rRNA processing. Studies of defective 27S pre-rRNA processing during Nop77p depletion show this type of generalized effect on the processing pathway (6).

Primer extension analysis of processing. Processing pathway alterations that lead to delayed formation of 25S rRNA may be accompanied by defects in processing site selection and may result in aberrant 5′ ends of intermediates in the processing pathway. To examine this possibility, primer extension was done to map the 5′ termini of pre-rRNAs that accumulate during Nop2p depletion, specifically at sites A_2, A_3, B_{1L}, and B_{1S} (locations of cleavage sites are shown in Fig. 4).

Endonucleolytic cleavages at sites A_2 and A_3 generate the 27SA intermediates (Fig. 9). The location of A_2 in L4717 is ACAAC | ACACU (Fig. 9A), which is the same position observed by Allmang et al. (1). Depletion of Nop2p for 8.5 h does not alter the fidelity of A_2 site selection or the extent of cleavage at this site compared to a *NOP2* strain. The 5′ end of the $27SA_3$ pre-rRNA is difficult to detect in this strain (Fig. 9A), making determination of the effect of Nop2p depletion problematic. Low ratios of $27SA_3$ to $27SA_2$ have been observed by others and may reflect strain differences (1). The only significant change in primer extension products that is attributed to Nop2p depletion is the detection of a small increase of an unusual cleavage site in ITS1, at position UUCGA | GCAAU (Fig. 9A).

Formation of the short and long 5.8S rRNAs involves two distinct processing pathways. The B_{1S} 5′ end is created by a combination of cleavage at A_3 followed by exonucleolytic digestion (18). The mechanism of B_{1L} 5′-end formation has not been established. The primer used detects 5′ ends of both 27S rRNA and 7S pre-rRNAs. The B_{1L} and B_{1S} 5′ ends in L4717 are located at UUAAA | AUAUUAA | AAACU, which are the same sites reported by Henry et al. (18). Depletion of Nop2p does not appear to have a significant effect on the formation of these 5′ ends (Fig. 9B). However, the ratio of B_{1S} to B_{1L}, which has been observed to be approximately 8 to 1 (18), appears to be reduced by Nop2p depletion (Fig. 9B).

Processing at C_1 generates the 5′ end of the 25S rRNA. In L4717, the 5′ end of the 25S rRNA is located at AAAGU |

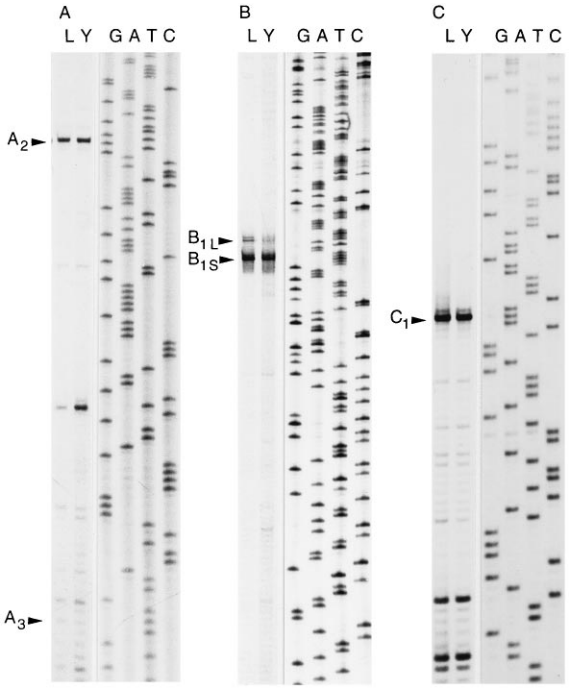

FIG. 9. Primer extension analysis of pre-RNAs during Nop2p depletion. Primer extensions were done with total RNA isolated from L4717 (*NOP2*; lanes L) or YBH5 (*GAL-NOP2*; lanes Y) grown for 8.5 h in SD medium. Oligonucleotide 3 (A), 9 (B), or 5 (C) was used. See Fig. 4 for the location of the oligonucleotides. DNA sequencing ladders were obtained with the same primers. Bands corresponding to the 5′ ends of pre-rRNAs generated by processing at sites A_2, A_3, B_{1L}, B_{1S}, and C_1 are indicated.

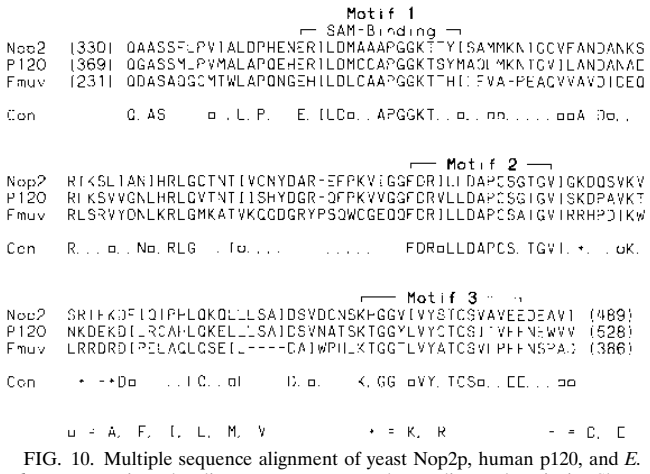

FIG. 10. Multiple sequence alignment of yeast Nop2p, human p120, and *E. coli* Fmuv proteins. The alignment was generated according to the Higgins-Sharp algorithm as implemented by MacDNASIS software. Amino acid numbers are indicated in parentheses. The full lengths of the Nop2p, p120, and Fmuv proteins are 618, 855, and 386 amino acids, respectively. A consensus sequence (Con) for the aligned stretch is shown, along with a key to the symbols used.

UUGAC (Fig. 9C). Depletion of Nop2p does not result in any detectable aberration in C_1 site selection (Fig. 9C).

Nop2p contains a putative SAM binding domain. Searches of the GenPept database with the Nop2p protein sequence revealed two proteins that show homology to Nop2p: human protein p120 and the product of the *E. coli fmuv* gene. Figure 10 shows the protein sequence alignment for Nop2p, p120, and the Fmuv protein in the region containing two motifs (1 and 2) present in known methylases (see reference 25). Motif 1 is thought to participate in binding of *S*-adenosylmethionine (SAM) and is present in a broad spectrum of methylases that modify proteins, nucleic acids, and lipid substrates (25). Also shown is a third motif (motif 3), which is positioned differently than in the article by Koonin (25) to highlight conserved positions that were not previously detected because *fmu* and *fmv* were previously considered to be separate genes in *E. coli*. Only a portion of the alignment of these three proteins is shown in Fig. 10. Significant homology (16% identity, 31% homology) between all three proteins extends approximately 104 amino acids toward the amino terminus of each protein, with the introduction of only three gaps in the Fmuv protein sequence (data not shown).

In an effort to address whether Nop2p is capable of binding SAM, we attempted to UV photo-cross-link SAM to Nop2p. A number of different assay conditions and different Nop2p-containing preparations (yeast nuclei, nuclear extracts, and two Nop2p–maltose-binding protein (MBP) fusion proteins purified from *E. coli*) were tried without success. The bacterially expressed methyltransferase domain from the vaccinia virus mRNA capping enzyme could be readily labeled when present by itself or after addition to the Nop2p-containing preparations. These results may be due to the absence of proper Nop2p conformation and/or posttranslational modification or the absence of proper intermolecular interactions (with a cofactor, substrate protein, and/or RNA).

Level of methylation of the conserved $UmGm\Psi UC_{2922}$ site remains low during Nop2p depletion. The observations that Nop2p depletion results in a specific defect in processing of 27S pre-rRNA and that Nop2p contains putative methylase motifs led us to consider the relationship between processing and methylation in the conversion of 27S pre-rRNA to 25S rRNA. The majority of the 67 methyl groups found in yeast rRNAs are added early, at the level of the 35S and 32S pre-rRNAs. Of the methylations found in the 25S rRNA, four are not present in the 35S or 32S pre-rRNAs and appear to be added late, at the level of the 27S precursor: two copies of 3-methyluracil and the doubly 2′-*O*-ribose-methylated sequence $UmGm\Psi UC_{2922}$ (8). The $UmGm\Psi UC_{2922}$ site lies near the 3′ end of domain 6; it is highly conserved in large-subunit RNA sequences from *E. coli*, yeast, and humans (16), and it has been implicated in peptidyl transfer (29).

To assay methylation, RNase protection was used to compare the amount of [^{3}H]methyl radioactivity incorporated at specific methylation sites in wild-type and Nop2p-depleted cells. RNase protection was done on samples labeled with [*methyl*-^{3}H]methionine and chased to incorporate label into the 27S pre-rRNA in YBH5. Oligonucleotide probes were used to protect a control site covering $m^1A_{643}AACAmCm$ (oligonucleotide 6), the $UmGm\Psi UC_{2922}$ site (oligonucleotide 7), and a control site covering $AmG_{2944}Cm$ (oligonucleotide 8) (Fig. 11A). Both control sites are methylated early (8). An important factor in this analysis is that depletion of Nop2p reduces incorporation of [*methyl*-^{3}H]methionine label into pre-rRNAs. Thus, the yield of protected [^{3}H]methylated RNAs from YBH5 will necessarily be lower than that from L4717. This is evident in T_1 partial digests of total [^{3}H]methylated RNAs from L4717 and YBH5 (Fig. 11C). We estimate that the difference in incorporation of label is two- to threefold, based on scintillation counting of bands from the T_1 digest gel (data not shown).

Comparison of the intensities of the bands from L4717 and YBH5 protected by control oligonucleotide 6 reveals a difference that is consistent with the reduction in efficiency of radiolabel incorporation after Nop2p depletion (Fig. 11B), as discussed above. A similar difference between L4717 and YBH5 is observed with control oligonucleotide 8 (Fig. 11B). Depletion of Nop2p in YBH5, however, results in a clear reduction in the intensity of the band protected by oligonucleotide 7 compared to that of the protected band from L4717 (Fig. 11B).

To evaluate differences in pre-rRNA methylation quantitatively, the radioactivity in protected [^{3}H]methylated RNAs was measured by scintillation counting. RNase protection was done in triplicate for this purpose. To correct for the difference in label incorporation discussed above, the data obtained from YBH5 were normalized by using the amount of radioactivity in the bands protected by control oligonucleotide 6. Oligonucleotide 6 was chosen as an internal standard because it protects three methyl groups that are added early and is located at a significant distance from the $UmGm\Psi UC_{2922}$ site. To evaluate oligonucleotide 6 as an internal standard, oligonucleotide 8 was used to protect another early-methylation site near $UmGm\Psi UC_{2922}$ (Fig. 11A). If oligonucleotide 6 is a valid internal standard for distinguishing between early and late methylation events, then no differences should be observed in the radioactivity values resulting from protection by oligonucleotide 8 after normalization.

In three independent experiments, the signal from YBH5 averaged only 66% (± 3%) of the control signal from L4717 (Table 3). In contrast, the radioactivity in the oligonucleotide 8-protected band from YBH5 was 97% (± 2%) of the amount of radioactivity from L4717 (Table 3). These data are consistent with what is observed by fluorography (Fig. 11B) and indicate that the level of methylation of the 27S pre-rRNA at $UmGm\Psi UC_{2922}$ remains low during Nop2p depletion. Thus, the delay in processing of 27S pre-rRNA incurred by Nop2p depletion is accompanied by a delay in methylation at the site $UmGm\Psi UC_{2922}$.

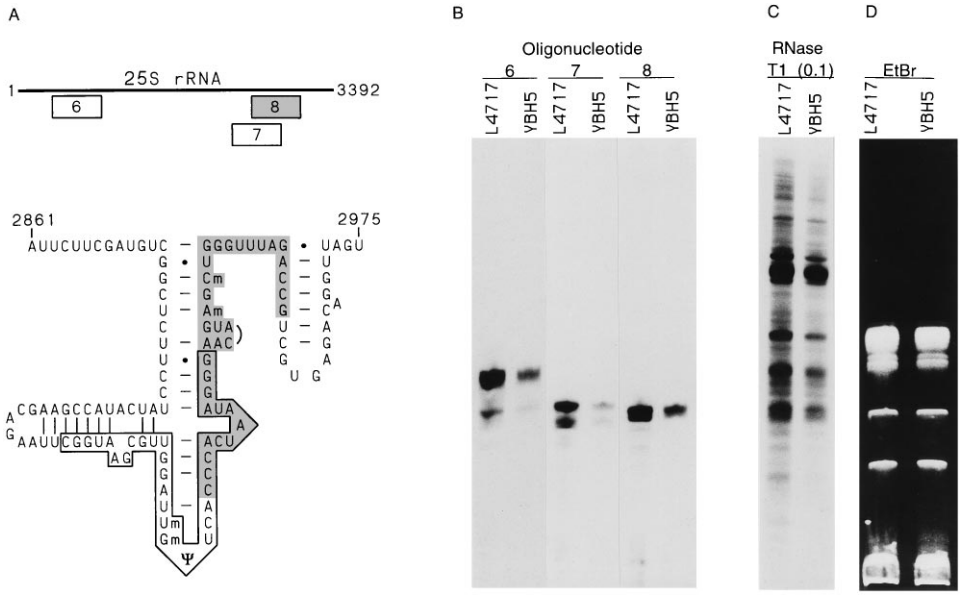

FIG. 11. RNase protection of ^{3}H-labeled rRNA. (A) Diagram of the 25S rRNA illustrating positions of oligonucleotides 6, 7, and 8. Oligonucleotide 7 is complementary to the boxed sequence, whereas oligonucleotide 8 is complementary to the shaded region. Oligonucleotide 6 is complementary to the stretch from nucleotide 635 to 674 (sequence not shown). Numbering of nucleotides is according to GenBank accession number K01048. (B) L4717 (*NOP2*) and YBH5 (*GAL-NOP2*) were grown on SD for 8.5 h and pulse-labeled with [*methyl*-^{3}H]methionine, and RNase protection was then performed. Protected fragments obtained with oligonucleotide 6, 7, or 8 were resolved in a 12% polyacrylamide–urea gel and visualized by fluorography. Oligonucleotide probes were not radioactivity labeled, and protected segments are radioactive by virtue of modification by one or more [^{3}H]methyl groups in rRNA. (C) Equivalent amounts of the same [^{3}H]RNA samples used for RNase protection were digested with RNase T_1 and electrophoresed on the same gel. (D) The same samples used for RNase protection were stained with ethidium bromide (EtBr).

The 33% reduction of methylation at $UmGm\Psi UC_{2922}$ is of a reasonable magnitude. Brand et al. observed that approximately 30% as much methyl label was present at $UmGm\Psi UC_{2922}$ in 27S pre-rRNA as was found in 25S rRNA (8). Also, perhaps only one of the two methyl groups in this stretch is added during processing of the 27S pre-rRNA.

A possible explanation for the reduced rate of processing and low level of methylation of 27S pre-rRNA is that 27S pre-rRNA is inefficiently converted to mature 25S rRNA that is not methylated at $UmGm\Psi UC_{2922}$. To examine this possibility, the methylation of 25S rRNA was assayed by a method that relies on the observation that low deoxynucleoside triphosphate concentrations induce reverse transcriptase to pause one nucleotide to the 3′ side of a 2′-*O*-ribose methylation on the template strand (32). This is referred to as a concentration-dependent pause (CDP) (32). CDPs in the 25S rRNA were assayed with a primer that is extended beginning with G_{2969} (see Fig. 11A). After Nop2p depletion, CDP bands that correspond to methylations at U_{2918} and G_{2919} were observed (data not shown). Likewise, CDP bands corresponding to ribose methylations in the stretch $GAmGCmU_{2946}$ and 3-methyluracil base methylation were also observed (data not shown). This indicates that Nop2p depletion does not result in a detectable reduction of methylation of $UmGm\Psi UC_{2922}$ in 25S rRNA. However, we can not exclude the possibility that 60S subunits are synthesized with undermethylated 25S rRNA but are unstable and degraded, which would prevent detection of undermethylated 25S rRNA in this assay.

DISCUSSION

To investigate the function of Nop2p, we constructed a strain in which the only copy of *NOP2* is under the control of the *GAL10* promoter. Growth in glucose medium represses Nop2p expression and dramatically lengthens cell doubling time. Nop2p depletion results in reduced steady-state levels of the 25S and 5.8S rRNAs found in the large subunit but has no significant effect on the 18S rRNA in the small subunit. Depletion of Nop2p diminished steady-state levels of 60S ribosomal subunits, monosomes, and polysomes. The level of the 40S subunit increased, leading to increases in 43S preinitiation complexes. Low levels of 25S and 5.8S rRNAs can be attributed to a defect in processing of 27S pre-rRNAs. Processing of 20S pre-rRNA to 18S rRNA was not significantly affected. The defect in 27S pre-rRNA processing does not appear to be due to abnormal processing within ITS1, such as alterations in cleavage site selection.

Protein sequence alignments identify Nop2p motifs present in methyltransferases. This raises the following question: what is the relationship between methylation and processing of 27S pre-rRNA? Methylation at the conserved site $UmGm\Psi UC_{2922}$ is thought to take place at the level of the 27S pre-rRNA (8), which is the level at which the Nop2p-dependent processing defect is observed. Thus, we examined methylation of this site and found that $UmGm\Psi UC_{2922}$ is not methylated in 27S pre-rRNA to the same extent that it is methylated in 25S rRNA. Low-level methylation of this site in 27S pre-rRNA is consistent with previous findings that 27S pre-rRNA is undermethylated at $UmGm\Psi UC_{2922}$ (8). The Nop2p-dependent delay in processing, which increases the half-life of the 27S pre-rRNA, is not accompanied by an increase in methylation despite the fact that there is sufficient time for methylation and processing of 27S pre-rRNA in control cells. Thus, depletion of Nop2p induces a significant delay in 27S pre-rRNA processing, which is accompanied by a delay in methylation as well. The concomitant reduction in both processing and methylation of 27S pre-rRNA suggests that these two events are closely interconnected during synthesis of 25S rRNA.

TABLE 3. RNase protection of ^{3}H-methylated rRNA

Expt	Protection afforded by:								
	Oligonucleotide 6[a]			Oligonucleotide 7			Oligonucleotide 8		
	L4717 dpm	Factor	%	L4717 dpm	YBH5 dpm	%	L4717 dpm	YBH5 dpm	%
1	3,929	2.57	100	2,163	1,522	70	3,124	3,058	98
2	1,423	3.27	100	723	471	65	716	699	98
3	975	2.19	100	334	214	64	325	307	95
Mean						66.3			97.0
Standard deviation (σ_{n-1})						3.2			1.7

[a] Oligonucleotide 6 was used as an internal standard, and a correction factor was used to normalize YBH5 DPM data for each experiment to 100%.

In addition to *NOP2*, a number of yeast gene products are known to be required for 60S subunit synthesis and production of 25S rRNA. Deficiencies in the products of genes *DRS1*, *NOP3*, *NOP4*/*NOP77*, *RPL1*, *RPL16B*, and *RRP1* lead to a specific reduction in the level of 25S rRNA, with little or no effect on 18S rRNA levels (6, 11, 13, 35, 38, 39, 46). However, the reduced rate of processing during Nop2p depletion is not accompanied by rapid turnover of 27S pre-rRNAs. With other gene products, except that of *RPL16B*, the 27S precursor is degraded in the absence of conversion to 25S rRNA. *RPL16B* is one of two homologous genes that encode the ribosomal protein L16. The 27S pre-rRNA is stable in the cold-sensitive allele *rpl16b-4* at 13°C; however, the two temperature-sensitive alleles *rpl16b-2* and *rpl16b-3* result in loss of both 25S and 27S species at 37°C (35). Thus, the relative stability of 27S pre-rRNA during Nop2p depletion is unusual with respect to known defects in 60S ribosomal subunit synthesis. Perhaps Nop2p depletion affects the ribosome assembly pathway at a point at which the 60S subunit is substantially complete and it is more efficient to arrest, rather than abort, the assembly process.

The consequences of Nop2p depletion suggest that processing and methylation during conversion of 27S pre-rRNA to 25S rRNA are coupled. One possible explanation for this is that Nop2p is required for 27S pre-rRNA processing because it functions as the methylase that modifies one or both of the riboses in the stretch $UmGm\Psi UC_{2922}$. However, because both processing and methylation occur during the conversion of 27S pre-rRNA to 25S rRNA, the effect of Nop2p depletion cannot be directly attributed to a methylation defect. For example, low-level methylation at $UmGm\Psi UC_{2922}$ in 27S pre-rRNA may be explained if methylation immediately follows processing, which is otherwise delayed by Nop2p depletion. Also, by analogy to Dim1p (29), it may be the presence of Nop2p, rather than its function, that is required for processing.

The line of investigation that we have followed raises interesting questions regarding the interdependence of processing and methylation. Does 27S pre-rRNA processing precede or follow methylation? Is there an obligate relationship between processing and methylation? A close temporal relationship between processing and methylation does not necessarily imply a cause-and-effect relationship. Recent studies in yeast cells suggest that methylation and processing are not obligatorily linked. The temperature-sensitive allele *nop1.3* inhibits methylation of 27S pre-rRNA at the nonpermissive temperature but does not substantially affect processing (50). This indicates that methylation is not required for processing or ribosome function. Dim1p is a methylase responsible for the conserved $m_2^6Am_2^6A$ modification in 18S rRNA, and depletion of Dim1p causes a defect in 20S pre-rRNA processing (26, 28). If the adjacent adenosines are replaced by guanine residues, processing proceeds normally in the absence of methylation, resulting in nonfunctional 40S subunits (26, 28). The presence of Dim1p is required for rRNA processing, but formation of the methylated residues is not directly monitored. Studies of the role of methylation in mammalian ribosome biogenesis, however, suggest that this modification is required for processing and function (9, 47, 53). Also, it is not clear if there are differences between early and late methylations in terms of their mechanism of synthesis or importance for ribosome function. Elucidation of the specific functional basis for the requirement for Nop2p in ribosome synthesis may shed light on the relationship between methylation and pre-rRNA processing during ribosomal subunit assembly.

ACKNOWLEDGMENTS

Bo Hong and Scott Brockenbrough contributed equally to this publication.

We are indebted to a number of colleagues who provided valuable advice on yeast molecular genetic techniques during the course of this work, especially James Anderson, Maurice Swanson, and John Woolford. We thank Cora Styles and Maurice Swanson for providing strains and plasmids. Alan Sachs suggested disrupting *NOP2* in a haploid strain transformed with complementing plasmid. Duanne Eichler, Alfred Lewin, and Gayle Knapp provided advice about RNase T_1 digestions and RNase protection assays. Eugene Koonin generously discussed motif analysis regarding Nop2p. Saeedur Khan kindly provided the absorbance monitoring instrumentation.

REFERENCES

1. **Allmang, C., Y. Henry, J. P. Morrissey, H. Wood, E. Petfalski, and D. Tollervey.** 1996. Processing of the yeast pre-rRNA at sites A(2) and A(3) is linked. RNA **2:**63–73.
2. **Anderson, J. T., S. M. Wilson, K. V. Datar, and M. S. Swanson.** 1993. NAB2: a yeast nuclear polyadenylated RNA-binding protein essential for cell viability. Mol. Cell. Biol. **13:**2730–2741.
3. **Ausubel, F. A., R. Brent, R. E. Kingston, D. D. Moore, J. G. Seidman, J. A. Smith, and K. Struhl (ed.).** 1996. Current protocols in molecular biology. Greene Publishing and Wiley-Interscience, New York.
4. **Baim, S. B., D. F. Pietras, D. C. Eustice, and F. Sherman.** 1985. A mutation allowing an mRNA secondary structure diminishes translation of *Saccharomyces cerevisiae* iso-1-cytochrome *c*. Mol. Cell. Biol. **5:**1839–1846.
5. **Bakin, A., and J. Ofengand.** 1995. Mapping of the 13 pseudouridine residues in *Saccharomyces cerevisiae* small subunit ribosomal RNA to nucleotide resolution. Nucleic Acids Res. **23:**3290–3294.
6. **Berges, T., E. Petfalski, D. Tollervey, and E. C. Hurt.** 1994. Synthetic lethality with fibrillarin identifies NOP77p, a nucleolar protein required for pre-rRNA processing and modification. EMBO J. **13:**3136–3148.
7. **Boeke, J. D., J. Truehart, G. Natsoulis, and G. R. Fink.** 1987. 5-Fluoroorotic acid as a selective agent in yeast molecular genetics. Methods Enzymol. **154:**164–175.
8. **Brand, R. C., J. Klootwijk, T. J. Van Steenbergen, A. J. De Kok, and R. J. Planta.** 1977. Secondary methylation of yeast ribosomal precursor RNA. Eur. J. Biochem. **75:**311–318.
9. **Caboche, M., J. P. Bachellerie.** 1977. RNA methylation and control of eukaryotic RNA biosynthesis. Effects of cycloleucine, a specific inhibitor of methylation, on ribosomal RNA maturation. Eur. J. Biochem. **74:**19–29.
10. **de Beus, E., J. S. Brockenbrough, B. Hong, and J. P. Aris.** 1994. Yeast *NOP2*

encodes an essential nucleolar protein with homology to a human proliferation marker. J. Cell Biol. **127:**1799–1813.
10a. **DeShaies, R. J.** Personal communication.
11. **Deshmukh, M., Y.-F. Tsay, A. G. Paulovich, and J. L. Woolford, Jr.** 1993. Yeast ribosomal protein L1 is required for the stability of newly synthesized 5S rRNA and the assembly of 60S ribosomal subunits. Mol. Cell. Biol. **13:**2835–2845.
12. **Eichler, D. C., and N. Craig.** 1995. Processing of eukaryotic ribosomal RNA. Prog. Nucleic Acid Res. Mol. Biol. **49:**197–239.
13. **Fabian, G. R., and A. K. Hopper.** 1987. *RRP1*, a *Saccharomyces cerevisiae* gene affecting rRNA processing and production of mature ribosomal subunits. J. Bacteriol. **169:**1571–1578.
14. **Freeman, J. W., J. E. Hazlewood, V. Bondada, M. L. Cibull, A. Fonagy, R. Ochs, R. K. Busch, and H. Busch.** 1989. Proliferation-related nucleolar antigens p145 and p120 associated with separate nucleolar elements and differences in tissue distribution. Cancer Commun. **1:**367–372.
15. **Girard, J. P., H. Lehtonen, F. M. Caizergues, F. Amalric, D. Tollervey, and B. Lapeyre.** 1992. GAR1 is an essential small nucleolar RNP protein required for pre-rRNA processing in yeast EMBO J. **11:**673–682.
16. **Gutell, R. R., M. W. Gray, and M. N. Schnare.** 1993. A compilation of large subunit (23S and 23S-like) ribosomal RNA structures: 1993. Nucleic Acids Res. **21:**3055–3074.
17. **Helser, T. L., R. A. Baan, and A. E. Dahlberg.** 1981. Characterization of a 40S ribosomal subunit complex in polyribosomes of *Saccharomyces cerevisiae* treated with cycloheximide. Mol. Cell. Biol. **1:**51–57.
18. **Henry, T., H. Wood, J. P. Morrissey, E. Petfalski, S. Kearsey, and D. Tollervey.** 1994. The 5′ end of yeast 5.8S rRNA is generated by exonucleases from an upstream cleavage site. EMBO J. **13:**2452–2463.
19. **Ito, H., Y. Fukuda, K. Murata, and A. Kimura.** 1983. Transformation of intact yeast cells treated with alkali cations. J. Bacteriol. **153:**163–168.
20. **Jansen, R., D. Tollervey, and E. C. Hurt.** 1993. A U3 snoRNP protein with homology to splicing factor PRP4 and G beta domains is required for ribosomal RNA processing. EMBO J. **12:**2549–2558.
21. **Jones, J. S., and L. Prakash.** 1990. Yeast *Saccharomyces cerevisiae* selectable markers in pUC18 polylinkers. Yeast **6:**363–366.
22. **Kiss-Laszlo, Z., Y. Henry, J.-P. Bachellerie, M. Caizergues-Ferrer, and T. Kiss.** 1996. Site-specific ribose methylation of preribosomal RNA: a novel function for small nucleolar RNAs. Cell **85:**1077–1088.
23. **Knapp, G.** 1989. Enzymatic approaches to probing of RNA secondary and tertiary structure. Methods Enzymol. **180:**192–212.
24. **Köhrer, K., and H. Domdey.** 1991. Preparation of high molecular weight RNA. Methods Enzymol. **194:**398–405.
25. **Koonin, E. V.** 1994. Prediction of an rRNA methyltransferase domain in human tumor-specific nucleolar protein p120. Nucleic Acids Res. **22:**2476–2478.
26. **Lafontaine, D., J. Delcour, A. L. Glasser, J. Desgres, and J. Vandenhaute.** 1994. The *DIM1* gene responsible for the conserved m(2)(6)Am(2)(6)A dimethylation in the 3′-terminal loop of 18 S rRNA is essential in yeast. J. Mol. Biol. **241:**492–497.
27. **Lafontaine, D., and D. Tollervey.** 1995. Trans-acting factors in yeast pre-rRNA and pre-snoRNA processing. Biochem. Cell Biol. **73:**803–812.
28. **Lafontaine, D., J. Vandenhaute, and D. Tollervey.** 1995. The 18S rRNA dimethylase Dim1p is required for pre-ribosomal RNA processing in yeast. Genes Dev. **9:**2470–2481.
29. **Lane, B. G., J. Ofengand, and M. W. Gray.** 1995. Pseudouridine and *O*-2′-methylated nucleosides. Significance of their selective occurrence in rRNA domains that function in ribosome-catalyzed synthesis of the peptide bonds in proteins. Biochimie **77:**7–15.
30. **Lee, W.-C., D. Zabetakis, and T. Mélèse.** 1992. NSR1 is required for pre-rRNA processing and for the proper maintenance of steady-state levels of ribosomal subunits. Mol. Cell. Biol. **12:**3865–3871.
31. **Maden, B. E.** 1988. Locations of methyl groups in 28 S rRNA of *Xenopus laevis* and man. Clustering in the conserved core of molecule. J. Mol. Biol. **201:**289–314.
32. **Maden, B. E., M. E. Corbett, P. A. Heeney, K. Pugh, and P. M. Ajuh.** 1995. Classical and novel approaches to the detection and localization of the numerous modified nucleotides in eukaryotic ribosomal RNA. Biochimie **77:**22–29.
33. **Maden, B. E. H.** 1990. The numerous modified nucleosides in eukaryotic ribosomal RNA. Prog. Nucleic Acid Res. Mol. Biol. **39:**241–303.
34. **Melese, T., and Z. Xue.** 1995. The nucleolus: an organelle formed by the act of building a ribosome. Curr. Opin. Cell Biol. **7:**319–324.
35. **Moritz, M., B. A. Pulaski, and J. L. Woolford, Jr.** 1991. Assembly of 60S ribosomal subunits is perturbed in temperature-sensitive yeast mutants defective in ribosomal protein L16. Mol. Cell. Biol. **11:**5681–5692.
36. **Nicoloso, M., L. H. Qu, B. Michot, and J. P. Bachellerie.** 1996. Intron-encoded, antisense small nucleolar RNAs: the characterization of 9 novel species points to their direct role as guides for the 2′-O-ribose methylation of rRNAs. J. Mol. Biol. **260:**178–195.
37. **Ripmaster, T. L., G. P. Vaughn, and J. L. Woolford, Jr.** 1992. A putative ATP-dependent RNA helicase involved in *Saccharomyces cerevisiae* ribosome assembly. Proc. Natl. Acad. Sci. USA **89:**11131–11135.
38. **Ripmaster, T. L., G. P. Vaughn, and J. L. Woolford, Jr.** 1993. *DRS1* to *DRS7*, novel genes required for ribosome assembly and function in *Saccharomyces cerevisiae*. Mol. Cell. Biol. **13:**7901–7912.
39. **Russell, I. D., and D. Tollervey.** 1992. NOP3 is an essential yeast protein which is required for pre-rRNA processing. J. Cell Biol. **119:**737–747.
40. **Segal, D. M., and D. C. Eichler.** 1991. A nucleolar 2′-O-methyltransferase. Specificity and evidence for its role in the methylation of mouse 28 S precursor ribosomal RNA. J. Biol. Chem. **266:**24385–24389.
41. **Sherman, F.** 1991. Getting started with yeast. Methods Enzymol. **194:**3–21.
42. **Sikorski, R. S., and J. D. Boeke.** 1991. In vitro mutagenesis and plasmid shuffling: from cloned gene to mutant yeast. Methods Enzymol. **194:**302–318.
43. **Sikorski, R. S., and P. Hieter.** 1989. A system of shuttle vectors and yeast host strains designed for efficient manipulation of DNA in *Saccharomyces cerevisiae*. Genetics **122:**19–27.
44. **Sirum-Connolly, K., and T. L. Mason.** 1993. Functional requirement of a site-specific ribose methylation in ribosomal RNA. Science **262:**1886–1889.
45. **Sollner-Webb, B., K. T. Tycowski, and J. A. Steitz.** 1996. Ribosomal RNA processing in eukaryotes, p. 469–490. *In* R. A. Zimmermann and A. E. Dahlberg (ed.), Ribosomal RNA: structure, evolution, processing, and function in protein synthesis. CRC Press, Boca Raton, Fla.
46. **Sun, C., and J. L. Woolford, Jr.** 1994. The yeast *NOP4* gene product is an essential nucleolar protein required for pre-rRNA processing and accumulation of 60S ribosomal subunits. EMBO J. **13:**3127–3135.
47. **Swann, P. F.** 1975. The effect of ethionine on ribonucleic acid synthesis in rat liver. Biochem. J. **150:**335–344.
48. **Tollervey, D.** 1987. A yeast small nuclear RNA is required for normal processing of pre-ribosomal RNA. EMBO J. **6:**4169–4175.
49. **Tollervey, D., H. Lehtonen, F. M. Carmo, and E. C. Hurt.** 1991. The small nucleolar RNP protein *NOP1* (fibrillarin) is required for pre-rRNA processing in yeast. EMBO J. **10:**573–583.
50. **Tollervey, D., H. Lehtonen, R. Jansen, H. Kern, and E. C. Hurt.** 1993. Temperature-sensitive mutations demonstrate roles for yeast fibrillarin in pre-rRNA processing, pre-rRNA methylation, and ribosome assembly. Cell **72:**443–457.
51. **Venema, J., and D. Tollervey.** 1995. Processing of pre-ribosomal RNA in *Saccharomyces cerevisiae*. Yeast **11:**1629–1650.
52. **Warner, J. R.** 1991. Labeling of RNA and phosphoproteins in *Saccharomyces cerevisiae*. Methods Enzymol. **194:**423–428.
53. **Wolf, S. F., and D. Schlessinger.** 1977. Nuclear metabolism of ribosomal RNA in growing, methionine-limited, and ethionine-treated HeLa cells. Biochemistry **16:** 2783–2791.
54. **Woolford, J. L., Jr., and J. R. Warner.** 1991. The ribosome and its synthesis, p. 587–626. *In* J. R. Broach, J. R. Pringle, and E. W. Jones (ed.), The molecular and cellular biology of the yeast *Saccharomyces*: genome dynamics, protein synthesis, and energetics, vol. I. Cold Spring Harbor Laboratory Press, Cold Spring Harbor, N.Y.